

Permian to Triassic protolith ages of type locality eclogites in the Eastern Alps: Implications for the opening of the Meliata back-arc basin

Ruihong Chang¹, Franz Neubauer^{1,*}, Yongjiang Liu^{2,*}, Johann Genser¹, Qingbin Guan², Qianwen Huang², and Sihua Yuan³

¹Department of Environment and Biodiversity, Paris Lodron University of Salzburg, 5020 Salzburg, Austria

²Frontiers Science Center for Deep Ocean Multispheres and Earth System, Key Lab of Submarine Geoscience and Prospecting Techniques, College of Marine Geosciences, Ocean University of China, Qingdao 266100, China

³China College of Earth Science, Institute of Disaster Prevention, Sanhe 065201, Hebei Province, China

ABSTRACT

The Austroalpine domain contains the type locality of eclogites, but their protolith age is unknown except for a Permian metagabbro. Therefore, we studied the non-gabbroic eclogites from the Saualpe-Koralpe Complex (SKC) representing meta-basalts within a coherent continental rift fragment subducted during the Cretaceous. Zircon laser ablation–inductively coupled plasma–mass spectrometry (LA-ICP-MS) U–Pb dating revealed protolith ages of 283 ± 5 Ma, 255 ± 3 Ma, 251 ± 3 Ma, and 241 ± 3 Ma. Magmatic zircons exhibit $^{176}\text{Hf}/^{177}\text{Hf}$ ratios of 0.282935–0.283090 and juvenile $\varepsilon_{\text{Hf}(t)}$ values of +10 to +17.4. Typical normal mid-oceanic ridge basalt (N-MORB) geochemistry is established. The SKC host metasedimentary rocks are interpreted as Variscan continental crust close to the margin of the oceanic Meliata basin and were affected by Permian metamorphism. Metamorphic zircon of one SKC eclogite yields an age of 87–93 Ma. These results combined with previous data are used to present a new model for the tectonic evolution of the distal Austroalpine unit associated with the Meliata Ocean in a Wilson cycle: The SKC represents a distal continental margin during Permian to Middle Triassic rifting, which was intruded by few gabbro bodies and numerous basaltic sills and mostly Permian pegmatites. In contrast, structurally separated thick Triassic sedimentary cover successions of the Austroalpine domain lack any magmatism, excluding SKC as Triassic basement of the sedimentary cover successions. The present eclogite-bearing piece of continental crust adjacent to the Meliata oceanic lithosphere was subducted to mantle depth during Late Cretaceous and then exhumed.

INTRODUCTION

Since the advent of plate tectonics, global subduction orogeny has continuously shaped the continents, accreting continental blocks and new crust at convergent plate boundaries. A prominent example of those processes is the breakup of the Gondwana supercontinent, the formation of intervening oceanic basins, and their subsequent consumption through subduction, which finally led to the formation of the Alpine-Himalayan orogenic belt. High-pressure to ultrahigh-pressure (HP-UHP) metamorphic

rocks like blueschists and eclogites are the specific products of subduction of oceanic or continental crust and provide information on their formation in the subduction channel (Peacock, 2003; Ernst and Liou, 2008; Roda et al., 2012; Penniston-Dorland et al., 2015; Agard, 2021). Continental and/or oceanic crustal and mantle rocks are typical components of exhumed subduction complexes. Therefore, these rocks record valuable information on subduction and exhumation processes (Guillot et al., 2009; Erdman and Lee, 2014; Lardeaux, 2014; Agard, 2021) and commonly form in the rift or drift setting, preserving information on the initiation and/or early stage of a Wilson cycle (e.g., Marotta and Spalla, 2007; Schuster and Stüwe, 2008; Roda et al., 2019).

The type area (Kupplerbrunn) of eclogites (Häüy, 1822) is hosted within the Saualpe-Koralpe Complex (SKC) of the Austroalpine units in the Eastern Alps, Europe (Figs. 1A and 1B). The SKC represents a coherent piece of subducted and exhumed continental crust (Schmid et al., 2004; Janák et al., 2015). Numerous petrological and geochronological studies have documented the metamorphic evolution of these eclogites and their surrounding rocks and established a Cretaceous age for HP-UHP metamorphism (Thöni and Jagoutz, 1992; Thöni and Miller, 1996; Thöni et al., 2008; Janák et al., 2015; Schorn et al., 2021). The protolith ages are however unknown except for the eclogitized Bärenfen metagabbro, for which three Permian to earliest Triassic Sm–Nd ages between 275 ± 18 and 247 ± 14 Ma have been reported (Thöni and Jagoutz, 1992; Miller and Thöni, 1997). Based on geochemical reasoning, Miller et al. (2005) suggested two types of eclogite precursor rocks: rare cumulate gabbros (in three locations only) and abundant rocks with a basaltic composition. The age of the latter remains unknown so far. Previous work reported also Permian high-temperature metamorphism related to lithospheric extension and subsequent Middle Triassic formation of the Adriatic passive continental margin and opening of the Tethys Ocean (Habler and Thöni, 2001; Schuster and Stüwe, 2008), but there are no age data for oceanic crust.

We present coupled zircon U–Pb age, trace element, and Lu–Hf isotopic data of non-gabbroic eclogites of basaltic composition from the SKC and report their protolith ages. The new data are integrated in a new model of opening and closure of the Meliata oceanic rift.

Ruihong Chang  <https://orcid.org/0000-0002-1326-3622>

*franz.neubauer@plus.ac.at; liyongjiang@ouc.edu.cn

CITATION: Chang, R., et al., 2023, Permian to Triassic protolith ages of type locality eclogites in the Eastern Alps: Implications for the opening of the Meliata back-arc basin: *Geology*, v. 51, p. 537–542, <https://doi.org/10.1130/G50903.1>

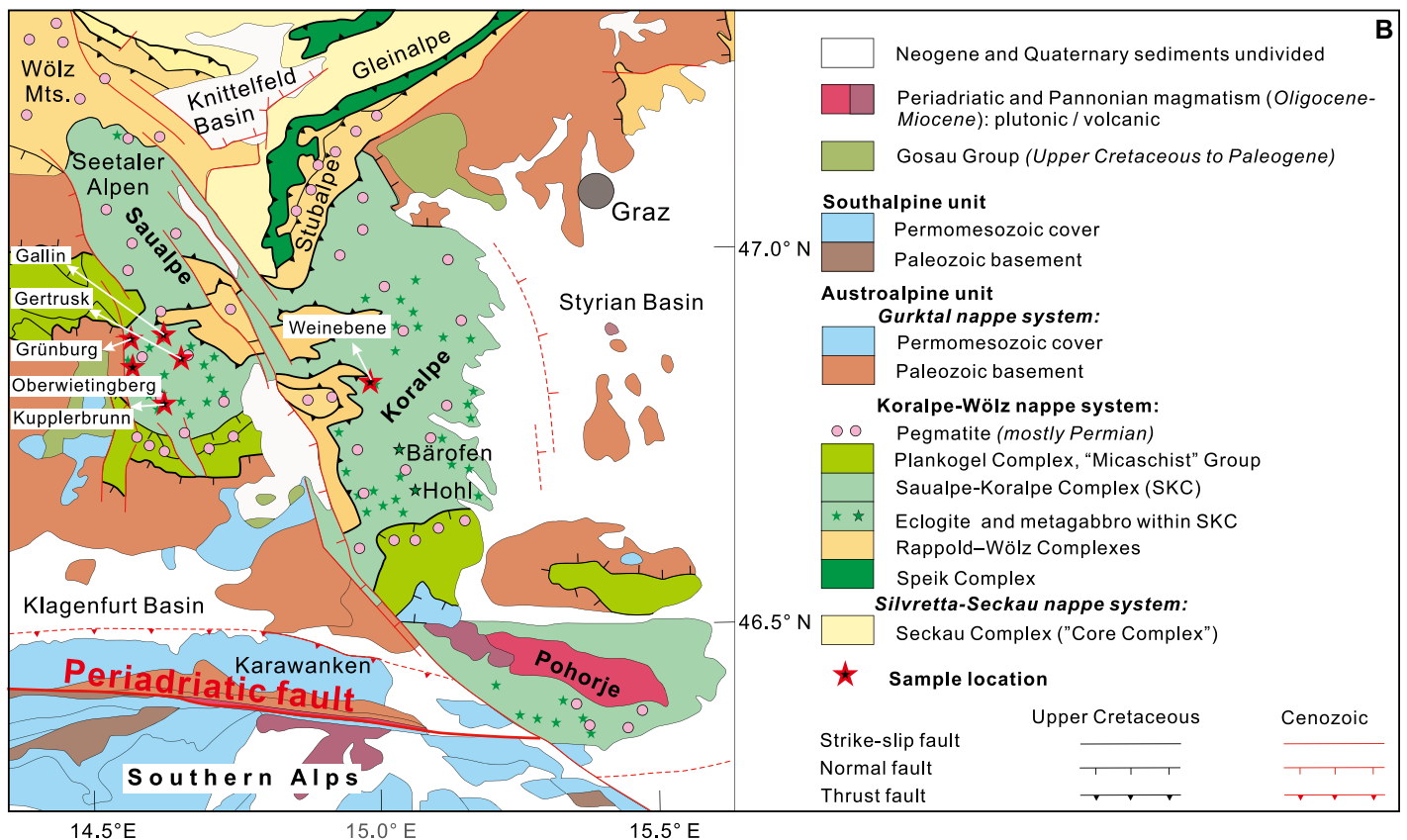
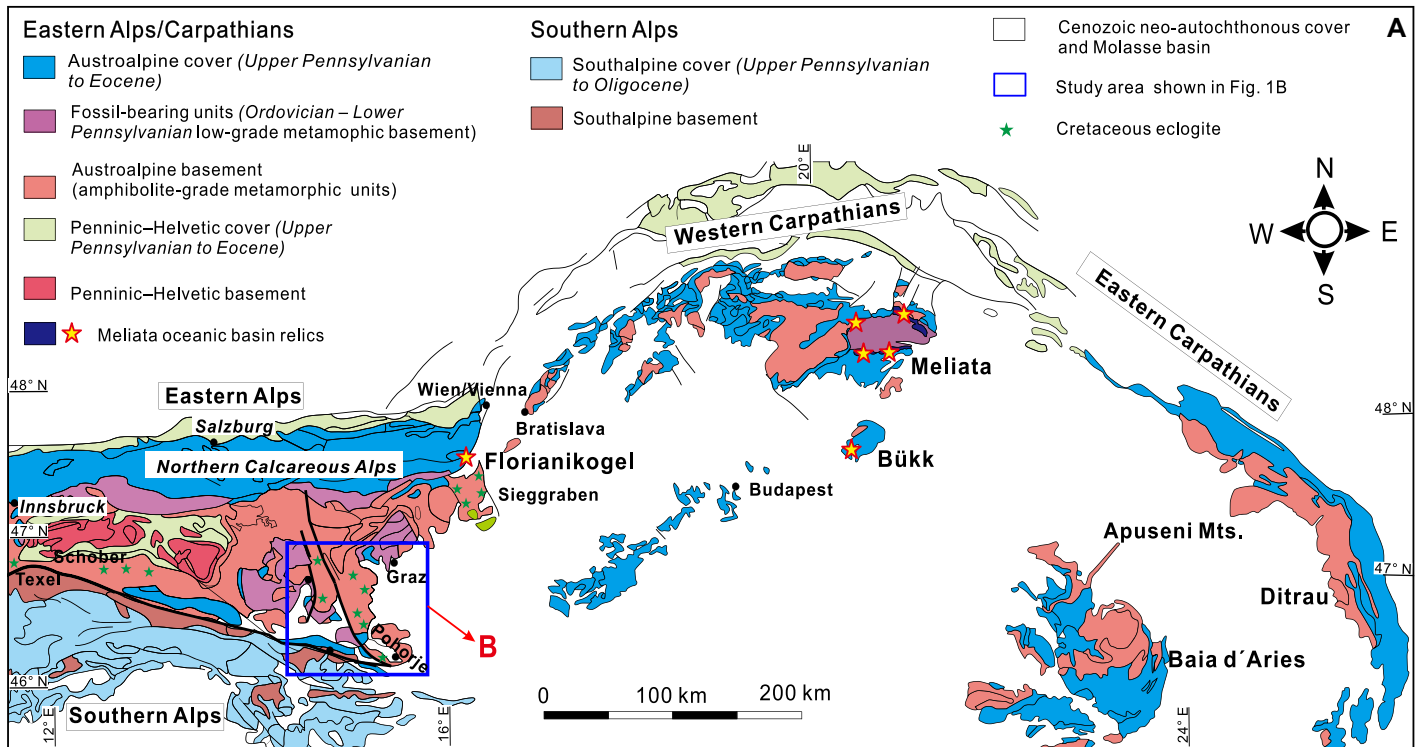


Figure 1. (A) Overview of the eastern part of the Eastern Alps and adjacent Carpathian area (Europe) illustrating distribution of Meliata Basin remnants and of Cretaceous eclogites. (B) Tectonic map of the Saualpe-Koralpe-Pohorje area indicating distribution of eclogites and Permian meta-pegmatites (after Chang et al., 2020).

OVERVIEW OF ECLOGITE-BEARING UNITS

In the eastern part of the Eastern Alps, several eclogite-bearing units can be recognized,

which are exposed in the Texel, Schober, Saualpe-Koralpe, Pohorje and Siegraben areas (Figs. 1A and 1B). Eclogites occur enclosed within metapelitic paragneisses (Roda et al.,

2012; Hauke et al., 2019; Chang et al., 2020; Miladinova et al., 2022) as lens-shaped bodies between one and several hundreds of meters in length.

The SKC is composed of metasedimentary rocks that experienced at least two metamorphic events: a Permian low-pressure–high-temperature (LP-HT) and an Eo-Alpine Cretaceous high-pressure–medium-temperature (HP-MT) event (Habler and Thöni, 2001; Schuster and Stüwe, 2008; Krenn et al., 2021). Metasedimentary rocks consist of variably deformed, staurolite- and/or aluminosilicate-bearing micaschists and paragneisses and contain numerous Permian pegmatite bodies (e.g., Knoll et al., 2018). Cretaceous subduction overprinted Permian SKC magmatic rocks (i.e., mafic rocks and pegmatites) and paragneisses, exemplified by kyanite paramorphoses after andalusite, by forming eclogites and lenses of foliation-parallel meta-pegmatites. The SKC is underlain and overlain by units of micaschist re-equilibrated under amphibolite-facies conditions (Rappold-Wölz and Plankogel Complexes; Fig. 1B), which lack any HP relics. The lower SKC boundary is a mylonitic thrust, the upper one a mylonitic low-angle normal fault (Wiesinger et al., 2006).

SAMPLES AND PETROLOGY

We collected 11 eclogite samples and one meta-pegmatite at six locations in the Saualpe and Koralpe (Fig. 1B; Table S1 in the Supplemental Material¹). The eclogites are composed of garnet (typical composition $\text{Prp}_{\sim 28}\text{Alm}_{\sim 45}\text{Grs}_{\sim 26}\text{Sps}_{\sim 1}$, where Prp is pyrope, Alm is almandine, Grs is grossular, and Sps is spessartine), omphacite (jadeite component $X_{\text{jd}} = 0.38\text{--}0.40$), phengite, paragonite, calcic to sub-calcic amphibole, zoisite, quartz, rutile, and ilmenite (Miller et al., 2005, and references therein). All samples display a well-equilibrated microfabric except for sample SA53A, which shows a secondary foliation and retrogressive quartz and plagioclase around garnet and omphacite leading to a migmatized appearance (Fig. S1). The peak metamorphic mineral assemblage is garnet + omphacite + phengitic white mica + quartz + rutile (Fig. S1).

METHODS

Details on the instrumentation, analytical procedure, data reduction for U-Pb laser ablation–inductively coupled plasma–mass spectrometry (LA-ICP-MS) geochronology, geochemistry of whole rocks, zircon

cathodoluminescence (CL) images, age spectra, photomicrographs, U-Pb ages, and Hf isotopic data for all samples are available in the Supplemental Material (Figs. S1–S5, Tables S2–S6, and supplemental text).

RESULTS

Zircon U-Pb Ages and Hf Isotopic Composition

Four eclogite samples yielded sufficient zircon grains for U-Pb dating. In CL images, selected grains in three eclogites (samples SA52A, SA53A, and SA55A) either reveal a weak oscillatory zoning or are homogeneous. They yielded U-Pb ages of 283.4 ± 5.1 Ma, 255.6 ± 3.5 Ma, 251.1 ± 3.1 Ma, and 241.0 ± 3.2 Ma (Fig. 2; Table S2). Sample SA52A includes two zircon populations: a younger one (241.0 ± 3.2 Ma), homogeneous in CL images, interpreted as the age of protolith crystallization, and an older one (255.6 ± 3.5 Ma) with oscillatory zoning interpreted as the age of xenocrystic zircons of an older crystallization event. In sample SA56A, zircon ages scatter around 250 Ma but without precise age. These zircons have relatively low and uniform U and Th concentrations ($3\text{--}203$ and $0.4\text{--}112$ $\mu\text{g/g}$, respectively) with Th/U ratios of $0.1\text{--}1.49$ typical for a magmatic origin, except for five grains ($\text{Th/U} < 0.1$) with homogeneous appearance in CL images suggesting a metamorphic origin. One eclogite (SA56A) yielded a 91.2 ± 1.2 Ma metamorphic age group and few grains with Middle Triassic to Permian ages. Sample SA53A has a small age group at 193.8 ± 3.3 Ma.

Hf Isotopic Composition of Zircons

The Hf isotopic composition of 35 zircons from four eclogites and one pegmatite allows separation of them into two groups (Fig. 2E). One group (samples SA52A, SA53A, and SA55A) yielded $\epsilon_{\text{Hf}(t)}$ values from $+10.0$ to $+14.5$ that straddle the mean value of the new crust (depleted mantle model age, T_{DM} , at $350\text{--}431$ Ma; Table S4; Fig. 2F). Sample SA56A has $\epsilon_{\text{Hf}(t)}$ from -1.4 to $+9.2$ in Permian ages corresponding to T_{DM} ages of $430\text{--}940$ Ma, suggesting a magma source that had an isotopic composition between mantle and crustal values or was influenced by the nearby pegmatite represented by sample SA57A. Other zircons from SA56A display $\epsilon_{\text{Hf}(t)}$ of $+4.5$ to $+5.8$ at ca. 91 Ma U-Pb age with T_{DM} ages of $513\text{--}570$ Ma, differing remarkably from the new crustal-type Hf isotope composition of Permian to Triassic protolith zircons from the eclogites.

Geochemistry

Eleven samples of non-gabbroic eclogites from six localities (Fig. 1B) were collected for whole-rock major and trace element analysis. Except for sample SA53A with a pronounced

secondary foliation, samples are similar in petrography, varying slightly in the amount of main minerals and microfabrics (Fig. S1). Only relatively immobile elements are used in the following discussion. Ten eclogite samples show uniform SiO_2 contents ranging from 47.15 to 49.74 wt%; only one migmatized eclogite (sample SA56A) has a higher SiO_2 content of 55.59 wt%. The rare earth elements (REEs) of eclogite samples are depleted in light REEs (Fig. 3B), with eight eclogites displaying $(\text{La}/\text{Lu})_{\text{N}}$ and $(\text{La}/\text{Yb})_{\text{N}}$ (N —normalized) values of $0.46\text{--}0.99$ and $0.43\text{--}0.97$ respectively; only two samples have ratios >1 [$(\text{La}/\text{Lu})_{\text{N}} = 1.25\text{--}1.47$ and $(\text{La}/\text{Yb})_{\text{N}} = 1.01\text{--}1.53$]. Sample SA56A gives $(\text{La}/\text{Lu})_{\text{N}}$ and $(\text{La}/\text{Yb})_{\text{N}}$ values of 5 and 4.92, respectively (Table S5). None of the samples exhibits an Eu anomaly, indicating their origin from basaltic liquids (Fig. 3B). Except for sample SA53A, all samples display uniform REE patterns and a typical normal mid-oceanic ridge basalt (N-MORB)-like positive slope (Fig. 3B). Sample SA53A has a light-REE-depleted pattern, explained as the result of secondary alteration.

On a Zr/Ti versus Nb/Y diagram, all eclogite samples plot within the basalt field, and on an AFM plot, most samples fall into the tholeiitic field (Figs. S5A and S5B). In the primitive mantle-normalized multi-element variation diagram (Fig. 3A), aside from the obvious N-MORB character, eclogites show enrichment in U, Pb, Nd, Sm, and Er and depletion in high-field-strength elements and large-ion lithophile elements such as Ba, Sr, Zr, and Hf.

DISCUSSION

Geochronological Constraints on Eclogites

The U-Pb ages obtained from three eclogites (samples SA52A, SA53A, and SA56A) define four mean $^{206}\text{Pb}/^{238}\text{U}$ ages of 283.4 ± 5.1 Ma, 255.6 ± 3.5 Ma, 251.1 ± 3.1 Ma, and 241.0 ± 3.2 Ma, from Permian to Middle Triassic. All dated zircons display Th/U ratios >0.1 . The REE patterns of zircons reveal that they are strongly depleted in light REEs relative to heavy REEs and show positive anomalies for Ce and slightly negative to no Eu anomalies in chondrite-normalized patterns. We consider that the age of 193.8 ± 3.3 Ma (sample SA53A) indicates hydrothermal alteration prior to metamorphic eclogite crystallization because of the homogenous CL pattern and low Th/U ratios ($0.125\text{--}0.147$). The interpretation is also supported by the distinct light REE-depleted pattern of this sample (Fig. 3B).

The metamorphic event at 91.2 ± 1.2 Ma identified in this study represents the age of eclogite metamorphism (e.g., Thöni et al., 2008). The calculated Zr saturation temperatures from eclogites are between 555 and 690 °C (Watson and Harrison, 1983) and $468\text{--}626$ °C (using parameters of Boehnke et al., 2013) and are in

¹Supplemental Material. Analytical methods with zircon U-Pb geochronology, geochemistry, and Hf isotopic analysis, and whole-rock geochemical analysis; sample locations, geochemical and isotopic data in (Tables S1–S7); microphotographs of studied eclogite samples, cathodoluminescence images, supplemental U-Pb and Hf isotopic plots of zircons, and supplemental whole rock geochemical plots. Please visit <https://doi.org/10.1130/GEOL.S.22280872> to access the supplemental material, and contact editing@geosociety.org with any questions.

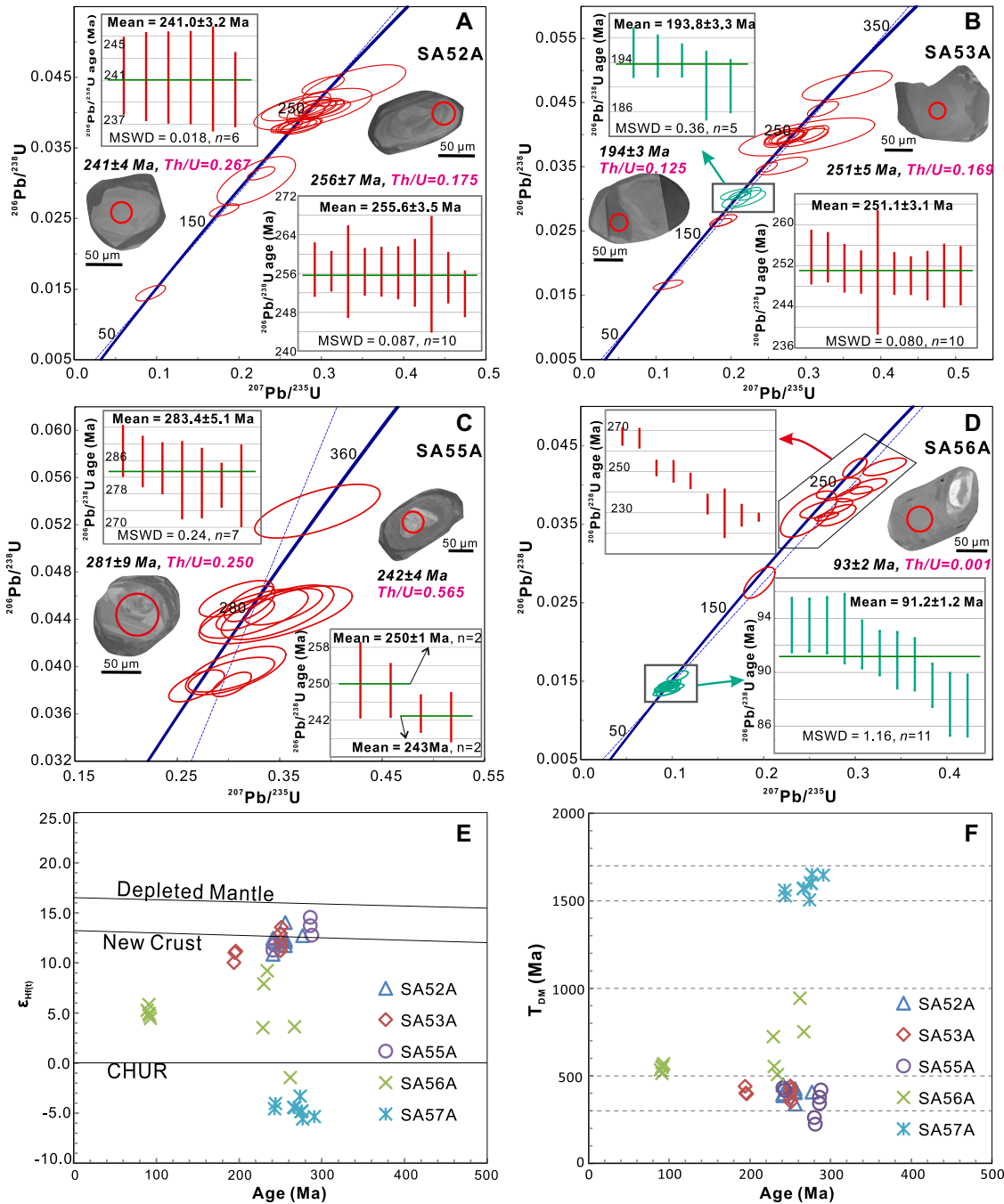


Figure 2. (A–D) Representative CL images, concordia plots of U–Pb zircon data, and inset plots of various $^{206}\text{Pb}/^{238}\text{U}$ mean age populations of eclogites. MSWD—mean square of weighted deviates. (E) Plots of $\epsilon_{\text{Hf}}(t)$ versus U–Pb age. CHUR—chondritic uniform reservoir. (F) Depleted mantle model age (T_{DM}) versus age of concordant zircons.

line with expected Cretaceous metamorphism with a maximum of 680 °C (Thöni et al., 2008).

In summary, the zircon U–Pb ages and Hf isotopes of eclogite samples SA52A, SA53A, and SA55A strongly suggest Permian to Middle Triassic magmatism marked by a dominant basaltic contribution from a juvenile mantle source. The temperature throughout the history of the SKC was insufficient to cause the loss of radiogenic daughter isotopes from zircons after their crystallization. The new U–Pb data, therefore, record the crystallization age of the eclogite protolith. Together with Hf isotope data and whole-rock geochemistry (see following discussion), these ages suggest previously unrecog-

nized basaltic emplacement events from Permian to Middle Triassic, in part significantly younger than the dated Permian metagabbro (Thöni and Jagoutz, 1992).

Origin of Eclogite Protoliths

Except for one sample (SA56A), the multi-element variation diagrams indicate that the SKC eclogites are tholeiitic basalt and/or N-MORB magmas contaminated by continental crust components, which may be the consequence of contamination of eclogite protoliths (i.e., basaltic liquids) prior to HP metamorphism or by surrounding migmatites during or after their emplacement.

Relationship between Eclogite Bodies and Pegmatites

Miller and Thöni (1997) estimated the emplacement conditions of the Permian gabbros at 0.17–0.29 GPa and 1000–1200 °C, indicating a shallow emplacement depth and implying overheating of immediate country rocks. The basaltic eclogites could have been emplaced as sills. In only a few cases, pegmatites are included into retrogressed eclogite.

The Permian extension event associated with abundant mafic and felsic igneous rocks is well known in the Austroalpine basement of the Eastern Alps (Schuster and Stüwe, 2008; Manzotti et al., 2018), in the Western Alps (Sesia zone; Manzotti

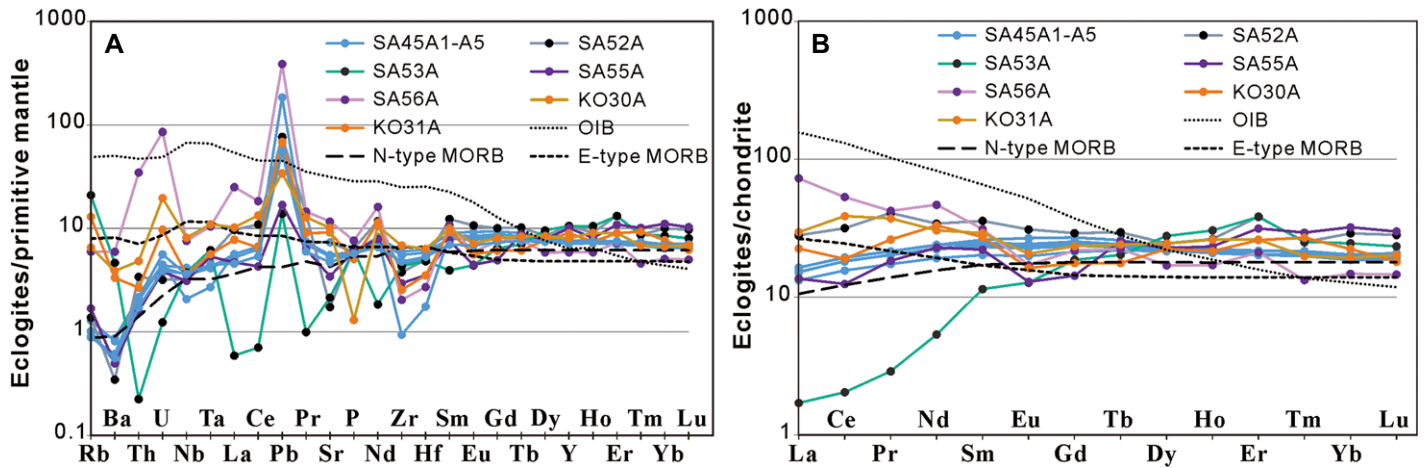


Figure 3. (A) Primitive mantle–normalized rare earth element (REE) patterns of eclogite samples (Sun and McDonough, 1989). (B) Chondrite-normalized REE patterns (normalized after Boynton, 1984). OIB—oceanic island basalt; N-type MORB, E-type MORB—normal- and enriched-type mid-oceanic ridge basalt, respectively.

et al., 2018), and in Southalpine units (Ivrea zone; Quick et al., 2009). Our new data indicate that the eastern part of the Austroalpine domain includes a much higher proportion of Permian to Middle Triassic mafic bodies than previously envisaged (Neubauer et al., 2022). For the SKC, emplacement of basaltic sills and gabbros led to partial melting of metasediments at mid-crustal levels along with LP amphibolite facies metamorphism. Anatectic melts are believed to have been the source for the pegmatites and granitoids that occur widely in the SKC (Knoll et al., 2018).

Tectonic Implications for the SKC and Regional Geology

The new data indicate that felsic and mafic Permian magmatism was more widespread

in the Austroalpine domain than previously assumed (Chang et al., 2020; Neubauer et al., 2022). In contrast to the Western Alps, evidence for Triassic magmatism in the Eastern Alps was entirely missing until now (Fig. 1B). Eclogite bodies make up a large percentage of SKC rocks. Accordingly, our new data reveal appreciable mafic magmatism in the SKC from the Permian to Middle Triassic, which corresponds to the extensional period predating the Ladinian (ca. 240 Ma) opening of the Meliata oceanic basin (e.g., Putiš et al., 2019). Given that magmatism is entirely missing within the thick, well-studied Permian–Mesozoic Austroalpine cover successions (Fig. 1A), our data cast doubt on the basement-cover relationship commonly invoked in tectonic models for the Eastern Alps.

Meliata-related basaltic rocks of Western Carpathians range in age from Early to Late Triassic (Putiš et al., 2019). Based on previous and new data from the Alps and Carpathians, we consider that the continental rifting started no earlier than 283 Ma, then progressed from the Late Permian to Middle Triassic between 255.6 ± 3.5 Ma and 241 ± 3 Ma. The ca. 283 Ma age of sample SA55A could represent captured zircons from older magmatic rocks such as pegmatites.

Based on our new data, the following tectonic model is proposed (Fig. 4): During the Permian to Middle Triassic, basaltic sills and rare Permian gabbros were emplaced into shallow levels of Austroalpine basement units. This part of the Austroalpine basement must have been located more distal to the future oceanic Meliata basin, typical for an asymmetric rift because of the restriction of the HT metamorphism (Schuster and Stüwe, 2008) to one side (Fig. 4A), now in the present-day footwall of the SKC. During Ladinian times, this rift developed to breakup and the opening of the Meliata back-arc basin (Putiš et al., 2019). After the Jurassic to Early Cretaceous consumption of the Meliata back-arc basin, the passive margin subducted to mantle depth (Fig. 4B) as envisaged by earlier authors (Janák et al., 2015).

A Late Permian to Middle Triassic

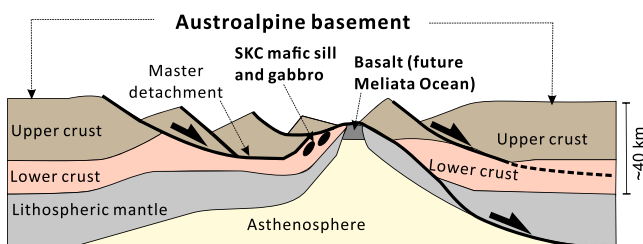
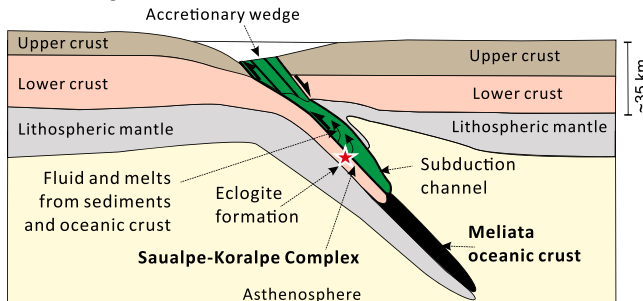


Figure 4. Tectonic model for the evolution of the Saualpe-Koralpe Complex (SKC). (A) Late Permian to Middle Triassic intrusion of basaltic sills and rare gabbros into shallow levels of distal Austroalpine basement units. (B) Late Cretaceous subduction of the SKC to mantle depths.

B Early Late Cretaceous



ACKNOWLEDGMENTS

We acknowledge critical comments by three anonymous reviewers and the editor, Urs Schaltegger, and thank Bianca Heberer for polishing the English. This study was financially supported by the National Natural Science Foundation of China (grant 9175212) to Liu and by a Ph.D. grant of the Chinese Scholarship Council (grant 201906170046) to Chang.

REFERENCES CITED

Agard, P., 2021, Subduction of oceanic lithosphere in the Alps: Selective and archetypal from (slow-spreading) oceans: *Earth-Science Reviews*, v. 214, 103517, <https://doi.org/10.1016/j.earscirev.2021.103517>.

- Boehnke, P., Watson, E.B., Trail, D., Harrison, T.M., and Schmitt, A.K., 2013, Zircon saturation revisited: *Chemical Geology*, v. 351, p. 324–334, <https://doi.org/10.1016/j.chemgeo.2013.05.028>.
- Boynton, W.V., 1984, Cosmochemistry of the rare earth elements: Meteorite studies, in Henderson, P., ed., *Rare Earth Element Geochemistry: Amsterdam, Elsevier, Developments in Geochemistry*, v. 2, p. 63–114, <https://doi.org/10.1016/B978-0-444-42148-7.50008-3>.
- Chang, R.H., Neubauer, F., Liu, Y.J., Genser, J., Jin, W., Yuan, S.H., Guan, Q.B., Huang, Q.W., and Li, W.M., 2020, Subduction of a rifted passive continental margin: The Pohorje case of Eastern Alps—Constraints from geochronology and geochemistry: *Swiss Journal of Geosciences*, v. 113, 14, <https://doi.org/10.1186/s00015-020-00369-z>.
- Erdman, M.E., and Lee, C.-T.A., 2014, Oceanic- and continental-type metamorphic terranes: Occurrence and exhumation mechanisms: *Earth-Science Reviews*, v. 139, p. 33–46, <https://doi.org/10.1016/j.earscirev.2014.08.012>.
- Ernst, W.G., and Liou, J.G., 2008, High- and ultrahigh-pressure metamorphism: Past results and future prospects: *American Mineralogist*, v. 93, p. 1771–1786, <https://doi.org/10.2138/am.2008.2940>.
- Guillot, S., Hattori, K., Agard, P., Schwartz, S., and Vidal, O., 2009, Exhumation processes in oceanic and continental subduction contexts: A review, in Lallemand, S., and Funicello, F., eds., *Subduction Zone Geodynamics: Berlin, Heidelberg, Springer*, p. 175–205, https://doi.org/10.1007/978-3-540-87974-9_10.
- Habler, G., and Thöni, M., 2001, Preservation of Permian-Triassic low-pressure assemblages in the Cretaceous high-pressure metamorphic Saualpe crystalline basement (Eastern Alps, Austria): *Journal of Metamorphic Geology*, v. 19, p. 679–697, <https://doi.org/10.1046/j.0263-4929.2001.00338.x>.
- Hauke, M., Froitzheim, N., Nagel, T.J., Miladinova, I., Fassmer, K., Fonseca, R.O.C., Sprung, P., and Münker, C., 2019, Two high-pressure metamorphic events, Variscan and Alpine, dated by Lu-Hf in an eclogite complex of the Austroalpine nappes (Schobergruppe, Austria): *International Journal of Earth Sciences*, v. 108, p. 1317–1331, <https://doi.org/10.1007/s00531-019-01708-8>.
- Häuy, R.J., 1822, *Traité de Minéralogie* (2nd edition): Paris, Bachelier et Huzard, 548 p.
- Janák, M., Froitzheim, N., Yoshida, K., Sasinková, V., Nosko, M., Kobayashi, T., Hirajima, T., and Vrabec, M., 2015, Diamond in metasedimentary crustal rocks from Pohorje, Eastern Alps: A window to deep continental subduction: *Journal of Metamorphic Geology*, v. 33, p. 495–512, <https://doi.org/10.1111/jmg.12130>.
- Knoll, T., Schuster, R., Huet, B., Mali, H., Onuk, P., Horschinegg, M., Ertl, A., and Giester, G., 2018, Spodumene pegmatites and related leucogranites from the Austroalpine Unit (Eastern Alps, Central Europe): Field relations, petrography, geochemistry, and geochronology: *Canadian Mineralogist*, v. 56, p. 489–528, <https://doi.org/10.3749/canmin.1700092>.
- Krenn, K., Husar, M., and Mikulics, A., 2021, Fluid and solid inclusions in host minerals of Permian pegmatites from Koralpe (Austria): Deciphering the Permian fluid evolution during pegmatite formation: *Minerals* (Basel), v. 11, 638, <https://doi.org/10.3390/min11060638>.
- Lardeaux, J.-M., 2014, Deciphering orogeny: A metamorphic perspective—Examples from European Alpine and Variscan belts: Part I, Alpine metamorphism in the western Alps—A review: *Bulletin de la Société Géologique de France*, v. 185, p. 93–114, <https://doi.org/10.2113/gssgfbull.185.2.93>.
- Manzotti, P., Rubatto, D., Zucali, M., El Korh, A., Cenk-Tok, B., Ballèvre, M., and Engi, M., 2018, Permian magmatism and metamorphism in the Dent Blanche nappe: Constraints from field observations and geochronology: *Swiss Journal of Geosciences*, v. 111, p. 79–97, <https://doi.org/10.1007/s00015-017-0284-1>.
- Marotta, A.M., and Spalla, M.I., 2007, Permian–Triassic high thermal regime in the Alps: Result of late Variscan collapse or continental rifting? Validation by numerical modeling: *Tectonics*, v. 26, TC4016, <https://doi.org/10.1029/2006TC002047>.
- Miladinova, I., Froitzheim, N., Nagel, T.J., Janák, M., Fonseca, R.O.C., Sprung, P., and Münker, C., 2022, Constraining the process of intracontinental subduction in the Austroalpine Nappes: Implications from petrology and Lu-Hf geochronology of eclogites: *Journal of Metamorphic Geology*, v. 40, p. 423–456, <https://doi.org/10.1111/jmg.12634>.
- Miller, C., and Thöni, M., 1997, Eo-Alpine eclogitisation of Permian MORB-type gabbros in the Koralpe (Eastern Alps, Austria): New geochronological, geochemical and petrological data: *Chemical Geology*, v. 137, p. 283–310, [https://doi.org/10.1016/S0009-2541\(96\)00165-9](https://doi.org/10.1016/S0009-2541(96)00165-9).
- Miller, C., Thöni, M., Konzett, J., Kurz, W., and Schuster, R., 2005, Eclogites from the Koralpe and Saualpe type-localities, eastern Alps, Austria: Mitteilungen der Österreichischen Mineralogischen Gesellschaft, v. 150, p. 227–263.
- Neubauer, F., Liu, Y.J., Dong, Y.P., Chang, R.H., Genser, J., and Yuan, S.H., 2022, Pre-Alpine tectonic evolution of the Eastern Alps: From Prototethys to Paleotethys: *Earth-Science Reviews*, v. 226, <https://doi.org/10.1016/j.earscirev.2022.103923>.
- Peacock, S.M., 2003, Thermal structure and metamorphic evolution of subducting slabs, in Eiler, J., ed., *Inside the Subduction Factory: American Geophysical Union Geophysical Monograph* 138, p. 7–22, <https://doi.org/10.1029/138GM02>.
- Penniston-Dorland, S.C., Kohn, M.J., and Manning, C.E., 2015, The global range of subduction zone thermal structures from exhumed blueschists and eclogites: Rocks are hotter than models: *Earth and Planetary Science Letters*, v. 428, p. 243–254, <https://doi.org/10.1016/j.epsl.2015.07.031>.
- Putiš, M., Soták, J., Li, Q.L., Ondrejka, M., Li, X.H., Hu, Z.C., Ling, X.X., Nemeč, O., Németh, Z., and Ružička, P., 2019, Origin and age determination of the Neotethys Meliata Basin ophiolite fragments in the Late Jurassic–Early Cretaceous accretionary wedge mélange (Inner Western Carpathians, Slovakia): *Minerals* (Basel), v. 9, 652, <https://doi.org/10.3390/min9110652>.
- Quick, J.E., Sinigoi, S., Peressini, G., Demarchi, G., Wooden, J.L., and Sbisà, A., 2009, Magmatic plumbing of a large Permian caldera exposed to a depth of 25 km: *Geology*, v. 37, p. 603–606, <https://doi.org/10.1130/G30003A.1>.
- Roda, M., Spalla, M.I., and Marotta, A.M., 2012, Integration of natural data within a numerical model of ablative subduction: A possible interpretation for the Alpine dynamics of the Austroalpine crust: *Journal of Metamorphic Geology*, v. 30, p. 973–996, <https://doi.org/10.1111/jmg.12000>.
- Roda, M., Regorda, A., Spalla, M.I., and Marotta, A.M., 2019, What drives Alpine Tethys opening? Clues from the review of geological data and model predictions: *Geological Journal*, v. 54, p. 2646–2664, <https://doi.org/10.1002/gj.3316>.
- Schmid, S.M., Fügenschuh, B., Kissling, E., and Schuster, R., 2004, Tectonic map and overall architecture of the Alpine orogen: *Eclogae Geologicae Helveticae*, v. 97, p. 93–117, <https://doi.org/10.1007/s00015-004-1113-x>.
- Schorn, S., Hartnady, M.I.H., Diener, J.F.A., Clark, C., and Harris, C., 2021, H₂O-fluxed melting of eclogite during exhumation: An example from the eclogite type-locality, Eastern Alps (Austria): *Lithos*, v. 390–391, <https://doi.org/10.1016/j.lithos.2021.106118>.
- Schuster, R., and Stüwe, K., 2008, Permian metamorphic event in the Alps: *Geology*, v. 36, p. 603–606, <https://doi.org/10.1130/G24703A.1>.
- Sun, S.-S., and McDonough, W.F., 1989, Chemical and isotopic systematics of oceanic basalts: Implications for mantle composition and processes, in Saunders, A.D., and Norry, M.J., eds., *Magmatism in the Ocean Basins: Geological Society, London, Special Publication* 42, p. 313–345, <https://doi.org/10.1144/GSL.SP.1989.042.01.19>.
- Thöni, M., and Jagoutz, E., 1992, Some new aspects of dating eclogites in orogenic belts: Sm-Nd, Rb-Sr and Pb-Pb isotopic results from the Austroalpine Saualpe and Koralpe type-locality (Carinthia/Styria, southeastern Austria): *Geochimica et Cosmochimica Acta*, v. 56, p. 347–368, [https://doi.org/10.1016/0016-7037\(92\)90138-9](https://doi.org/10.1016/0016-7037(92)90138-9).
- Thöni, M., and Miller, C., 1996, Garnet Sm-Nd data from the Saualpe and the Koralpe (Eastern Alps, Austria): Chronological and P-T constraints on the thermal and tectonic history: *Journal of Metamorphic Geology*, v. 14, p. 453–466, <https://doi.org/10.1046/j.1525-1314.1996.05995.x>.
- Thöni, M., Miller, C., Blicher-Toft, J., Whitehouse, M.J., Konzett, J., and Zanetti, A., 2008, Timing of high-pressure metamorphism and exhumation of the eclogite type-locality (Kupplerbrunn–Prickler Halt, Saualpe, southeastern Austria): Constraints from correlations of the Sm-Nd, Lu-Hf, U-Pb and Rb-Sr isotopic systems: *Journal of Metamorphic Geology*, v. 26, p. 561–581, <https://doi.org/10.1111/j.1525-1314.2008.00778.x>.
- Watson, E.B., and Harrison, T.M., 1983, Zircon saturation revisited: Temperature and composition effects in a variety of crustal magma types: *Earth and Planetary Science Letters*, v. 64, p. 295–304, [https://doi.org/10.1016/0012-821X\(83\)90211-X](https://doi.org/10.1016/0012-821X(83)90211-X).
- Wiesinger, M., Neubauer, F., and Handler, R., 2006, Exhumation of the Saualpe eclogite unit, Eastern Alps: Constraints from ⁴⁰Ar/³⁹Ar ages and structural investigations: *Mineralogy and Petrology*, v. 88, p. 149–180, <https://doi.org/10.1007/s00710-006-0154-4>.

Printed in USA